Title: Genome-wide mapping identifies beta-1,4-N-acetyl-galactosaminyl-transferase as a novel determinant of sclerostin levels and bone mineral density

Jie Zheng[1]+, Winfried Maerz[2,3,4], Ingrid Gergei[4], Marcus Kleber[4], Christiane Drechsler[5], Christoph Wanner[5], Vincent Brandenburg[5], Sjur Reppe[6,7], Kaare M Gautvik[7,8], Carolina Medina-Gomez[9], Enisa Shevroja[9], Arthur Gilly[10,11], Young-Chan Park[10,12], George Dedoussis[13], Eleftheria Zeggini[10,11], Mattias Lorentzon[14,15,16], Petra Henning[14], Ulf H. Lerner[14], Karin Nilsson[14], Sofia Movérare-Skrtic[14], Denis Baird[1], Louise Falk[1], Alix Groom[1,17], Terence D. Capellini[18,19], Elin Grundberg[20,21], Maria Nethander[14], Claes Ohlsson[14], George Davey Smith[1]*, Jonathan H. Tobias[22]*+

*Equal contributions

+ Corresponding author

[1]MRC Integrative Epidemiology Unit (IEU), Bristol Medical School, University of Bristol, Oakfield House, Oakfield Grove, Bristol, BS8 2BN, United Kingdom

[2]Clinical Institute of Medical and Chemical Laboratory Diagnostics, Medical University of Graz, Austria

[3]SYNLAB Academy, SYNLAB Holding Deutschland GmbH, Mannheim, Germany

[4]Vth Department of Medicine (Nephrology, Hypertensiology, Rheumatology, Endocrinology, Diabetology), Medical Faculty Mannheim, University of Heidelberg, Mannheim, Germany

[5]Department of Internal Medicine 1, Division of Nephrology and the Comprehensive Heart Failure Center, University of Würzburg, Germany

[6]Institute of Basic Medical Sciences, University of Oslo. Oslo, Norway

[7]Unger-Vetlesen Institute, Lovisenberg Diaconal Hospital, Oslo, Norway

[8]Department of Medical Biochemistry, Oslo University Hospital, Oslo, Norway

[9]Department of Internal Medicine, Erasmus MC University Medical Center, Rotterdam, The Netherlands

[10]Human Genetics, Wellcome Sanger Institute, Wellcome Genome Campus, Hinxton, CB10 1SA, United Kingdom

[11]Institute of Translational Genomics, Helmholtz Zentrum München, German Research Center for Environmental Health, Neuherberg, Germany

[12]University of Cambridge, Cambridge, UK

[13]Department of Nutrition and Dietetics, School of Health Science and Education, Harokopio University, El. Venizelou 70, 17671, Athens, Greece

[14]Centre for Bone and Arthritis Research, Department of Internal Medicine and Clinical Nutrition, Institute of Medicine, University of Gothenburg, Sweden

[15]Geriatric Medicine, Institute of Medicine, University of Gothenburg, Sweden

[16]Geriatric Medicine Clinic, Sahlgrenska University Hospital, Mölndal, Sweden

[17]Bristol Bioresource Laboratories, Population Health Sciences, Bristol Medical School, University of Bristol, UK

[18]Human Evolutionary Biology, Harvard University, USA

[19]Broad Institute of MIT and Harvard, USA

[20]Department of Human Genetics, McGill University, Quebec, Canada

[21]Center for Pediatric Genomic Medicine, Children's Mercy Kansas City, USA

[22]Musculoskeletal Research Unit, University of Bristol, Level 1 Learning and Research Building, Bristol, BS10 5NB, United Kingdom

ABSTRACT

In bone, sclerostin is mainly osteocyte-derived and plays an important local role in adaptive responses to mechanical loading. Sclerostin is also present at detectable concentrations within the circulation. Our genome wide association study (GWAS) meta-analysis of 10,584 European-descent individuals identified two novel serum sclerostin loci, *B4GALNT3* (standard deviation (SD) change in sclerostin per A allele β=0.20, P=4.6x10^{-49}), and *GALNT1* (β=0.11 per G allele, P=4.4x10^{-11}), of which the former is a known locus for BMD estimated by heel ultrasound (eBMD). Common variants across the genome explained 16% of the phenotypic variation of serum sclerostin. Mendelian randomization revealed an inverse causal relationship between serum sclerostin and femoral neck BMD and eBMD, and a positive relationship with fracture risk. Colocalization analysis demonstrated common genetic signals within the *B4GALNT3* locus for higher sclerostin, lower BMD, and greater *B4GALNT3* expression in arterial tissue (Probability>99%). Renal and cortical bone tissue, and osteoblast cultures, were found to express high levels of B4GALNT3, an N-acetyl-galactosaminyltransferase which adds a terminal LacdiNAc disaccharide to target glycocoproteins. Together, these findings raise the possibility that sclerostin is a substrate for B4GALNT3, such that its modification leads to higher levels, possibly through greater stability. *GALNT1*, an enzyme causing mucin-type O-linked glycosylation, may act in a similar capacity. We conclude that genetic variation in glycosylation enzymes represents a novel determinant of BMD and fracture risk, acting via alterations in levels of circulating sclerostin.

Introduction

Sclerostin is a glycoprotein produced by osteocytes, which is thought to play an important role in bone's adaptive response to mechanical loading, acting within the local bone microenvironment to suppress bone formation (1). The sclerostin antibody romosozumab has recently been found to increase bone mineral density (BMD) and reduce fracture risk (2)(3), establishing sclerostin as an important drug target for osteoporosis. Sclerostin is also detectable in the systemic circulation, the functional role of which remains unclear. Serum sclerostin exchanges with the bone micro-environment, and may simply mirror the prevalent conditions within bone. Consistent with this suggestion, serum sclerostin has been found to respond to physiological stimuli such as estrogen in parallel to alterations in local bone expression (4).

Several studies suggest that serum sclerostin exerts other roles outside the skeleton. For example, serum sclerostin has been reported to increase in chronic kidney disease (CKD), and may contribute to the pathogenesis of Chronic Kidney Disease–Mineral and Bone Disorder (CKD-MBD) (5). Serum sclerostin levels are also higher in patients with cardiovascular disease and may predict cardiovascular mortality (6). A relationship with glucose metabolism has been suggested in light by reports of higher sclerostin levels in association with type I and type II diabetes mellitus in adolescents (7) and adults (8) respectively. While these changes may represent 'off target' effects of sclerostin originating from bone, alternatively, sclerostin might act as an endocrine hormone, subject to regulation by as yet unidentified additional factors. Adding to this complexity, several extra skeletal tissues have been found to express sclerostin, including the liver, chondrocytes, kidney and vascular smooth muscle cells (9). Aside from extra skeletal target tissues, perturbations in serum sclerostin could conceivably affect the bone itself through consequent alterations of sclerostin levels within the local bone environment.

In order to identify novel factors affecting bone metabolism and other systems through altered sclerostin levels, we performed a genome wide association study (GWAS) meta-analysis of serum sclerostin. We then applied our results in a Mendelian randomization (MR) framework (10) to explore putative causal relationships between serum sclerostin and bone metabolism (as reflected by BMD).

RESULTS

Genome-wide association study meta-analysis of serum sclerostin

GWAS results were available in 10,584 participants across four cohorts (see Table 1). Supplementary Figures 1 and 2 show the Manhattan plot and QQ plot of association results from the fixed-effect meta-analysis of sclerostin in Europeans, respectively (see Supplementary Figure 3 for the QQ plots for each study). There was little evidence of inflation of the association results as the genomic inflation factors λ is 1.051 and the LD score regression intercept is 1.015 (11). Therefore, genomic control correction was not applied to any of the meta-analysis results. LD score regression revealed that all common variants we included in the meta-analysis explained 16.3% of the phenotypic variance of sclerostin (H^2=0.163, S.E.=0.052, P=0.0017)

Two loci were identified to be associated with serum sclerostin at a genome-wide level. 69 SNPs in the *B4GLANT3* gene region were associated with sclerostin level (Figure 1A). The top hit rs215226 at this locus (β = 0.205 SD change in serum sclerostin per A allele, SE = 0.014, P = 4.60 x 10^{-49} , variance explained = 1.99%) was previously reported to be associated with BMD estimated by heel ultrasound (eBMD) (12). The second locus was in the *GALNT1* gene region (Figure 1B) with the top hit rs7241221 (β = 0.109 SD per G allele, SE = 0.017, P = 4.40 x 10^{-11}, variance explained = 0.39%). In addition, one SNP near the *TNFRSF11B* region encoding OPG, rs1485303, was marginally associated with sclerostin (β = 0.074 SD per G allele, SE = 0.014, P = 7.70 × 10^{-8}, variance explained = 0.26%) (Figure 1C). The latter SNP is in moderate LD with a previously reported BMD associated SNP rs1353171 (r^2=0.277 in the 1000 Genome Europeans) (13). The association signals of the GWAS meta-analysis can be found in Table 2 and Supplementary Table 1. Results of the random effects meta-analysis were identical to those of the fixed effects meta-analysis (results not shown). The degree of heterogeneity was low across studies for the *GALNT1* signal (I^2=0) and *TNFRSF11B* signal (I^2=0.53) but relatively high for *B4GALNT3* signal (I^2=0.78) (Supplementary Table 2). The latter appeared to reflect a relatively strong association in 4D, suggesting as possible interaction with the presence of CKD. Conditional analyses on the lead SNP in each association locus yielded no additional independent signals reaching genome-wide significance.

Only minor genetic influences on serum sclerostin were observed within the *SOST* gene (Chromosome 17, 41731099 to 41936156), which produces sclerostin. In total, four *SOST* SNPs have previously been reported in association with BMD (12)(14), and one with fracture (15). However, proxy SNPs for these SNPs showed little or no association with serum sclerostin (Supplementary Table 3). We used the GWAS results to estimate the genetic correlation between sclerostin and 11 bone phenotypes using LD score regression via LD Hub (16). We observed no strong evidence of genetic correlation between sclerostin SNPs and the bone phenotypes we tested. (Supplementary Table 4).

Mendelian randomization and colocalization analysis of sclerostin and bone phenotypes

Using two sample Mendelian Randomization (MR), we applied our GWAS results to larger datasets in order to examine putative causal relationship between sclerostin and bone phenotypes. The two SNPs robustly associated with sclerostin (rs215226 in *B4GALNT3* region and rs7241221 in *GALNT1* region) were used as genetic instruments of the exposure. DXA-derived BMD and eBMD results from the GEFOS consortium (17) and UK Biobank (12) respectively, and fracture from UK Biobank, were used as outcomes. Contrasting with the genetic correlation results, based on inverse variance weighted (IVW) analysis, we observed that higher level of serum sclerostin was causally related to lower femoral neck BMD (β= -0.123 SD change in BMD per SD increase in sclerostin, 95%CI= -0.195 to -0.051, P=0.00074), lower eBMD (β= -0.122 SD change in BMD per SD increase in sclerostin, 95%CI= -0.140 to -0.104, P= 1.29×10^{-38}) and higher fracture risk (β=1.117 SD change in odds ratio (OR) per SD increase in sclerostin, 95%CI= 1.009 to 1.237, P= 0.034) (Figure 2). There was also weak evidence of an inverse relationship between sclerostin level and lumbar spine BMD. The single SNP MR results suggested that both instruments contributed to the overall causal effects we observed (Supplementary Table 5). Heterogeneity analysis of the instruments suggested that causal estimates were consistent across both SNPs (P values of Cochran Q test > 0.05), with the exception of estimates for lumbar spine BMD and fracture risk, likely reflecting the lower power in these instances (18). Colocalization analysis between sclerostin and eBMD suggested that both instruments colocalized with eBMD independently (PP=99.7% for the *B4GALNT3* locus and 99.8% for the *GALNT1* locus) (Supplementary Table 6), further strengthening the evidence of the putative causal relationship between sclerostin and eBMD.

We also undertook bidirectional MR (19) to evaluate the possibility of reverse causality between femoral neck BMD (or lumbar spine BMD) and serum sclerostin level, based on SNPs identified in GEFOS (17). We modelled femoral neck BMD and lumbar spine BMD as our exposure and serum sclerostin level as our outcome. The Steiger filtering analysis (20) suggested that 28 of the 32 femoral neck BMD SNPs and all 27 lumbar spine BMD SNPs exerted their primary effect on BMD as opposed to sclerostin (Supplementary Table 7). IVW results using 28 femoral neck BMD SNPs suggested a positive relationship between femoral neck BMD and sclerostin (β=0.157 SD change in sclerostin per SD change in BMD, 95%CI= 0.039 to 0.274, P=0.009) while IVW results using 27 lumbar spine BMD SNPs suggested a positive relationship between lumbar spine BMD and sclerostin (β=0.210 SD change in sclerostin per SD change in BMD, 95%CI=0.084 to 0.335, P=0.001). Sensitivity analyses using MR Egger and Weighted Median methods showed similar albeit weaker causal effects (Supplementary Table 8 and Supplementary Figure 4A and 4B). There was no strong evidence of horizontal pleitropy for femoral neck BMD (Egger regression intercept = -0.0082, P = 0.406) or lumbar spine BMD (Egger regression intercept = -0.0082, P = 0.511). The heterogeneity test suggested no strong heterogeneity across instruments for femoral neck (Cochrane Q = 34.397, P = 0.155), but suggested some heterogeneric effects across instruments for lumbar spine BMD (Cochrane Q = 40.132, P = 0.038). We further detected one outlier SNP for lumbar spine BMD using Cochrane test implemented in "RadialMR" R package (21)(22). The radial plot can be found in Supplementary Figure 5. As a sensitivity analysis, we removed the outlier SNP and IVW results using the remaining 26 lumbar spine BMD SNPs still suggested a positive relationship between lumbar spine BMD and sclerostin (β=0.244, 95%CI=0.123 to 0.365, P=8.02x10^{-5}) (Supplementary Table 8).

Functional follow-up

Predicted regulatory elements of the top association signals

We identified DNA features and regulatory elements of SNPs in high LD with the top association signals (r^2>0.8), using Regulomedb (23). Among the 24 tested SNPs, we found three proxy SNPs showing high Regulomedb score (Supplementary Table 9): rs1872426 (r^2=0.87 with the leading SNP rs1485303 in the *TNFRSF11B* region) had a score of 1f (eQTL + TF binding / DNase peak); rs215224 and rs4980826 (r^2=1 and 0.85 with the leading SNP rs215226 respectively in the *B4GALNT3* region) had a score of 2b (TF binding + any motif + DNase Footprint + DNase peak) (see Supplementary Figure 6 for rs215224). We also

intersected variants with ATAC-seq data (24) (25) generated from the proximal and distal femur (26). In the *TNFRSF11B* locus, one SNP, rs2073618, overlapped with an ATAC-seq peak, while in the *B4GALNT3* locus, four SNPs (rs12318530, rs215223, rs215224 and rs215225) fell in the same ATAC-Seq and Chip-Seq peak (Supplementary Figure 7 and Supplementary Table 10).

Expression QTLs lookups for sclerostin signals

To evaluate if the sclerostin association signals influence transcription of cis genes, we cross-referenced the sclerostin SNPs with *cis*-expression data in tissues measured in the GTEx consortium v7 (27), primary osteoblast cell lines (28) and iliac crest bone biopsies (29). The top association signal within the *B4GALNT3* region, rs215226, showed a strong positive association with *B4GALNT3* gene expression in arterial and ovarian tissue (Supplementary Table 11). In contrast, a weaker inverse association with *B4GALNT3* expression was observed in nervous tissue. Colocalization analysis yielded strong evidence that sclerostin levels share the same causal variant at this locus with arterial and ovarian *B4GLANT3* expression (probability > 99%), whereas there was no evidence of co-localisation in the case of nervous tissue (Supplementary Table 12). The association signal in the *GALNT1* region was positively associated with *GALNT1* expression in adipose tissue, and that of the neighbouring gene, *INO80C*, in adipose and heart tissue. In contrast, sclerostin association signals in *B4GALNT3*, *TNFRSF11B* and *GALNT1* were not associated with *cis*-regulation of mRNA expression in osteoblast cells (Supplementary Table 13) or iliac crest bone biopsies (Supplementary Table 14). In *trans*-eQTL analyses, the *GALNT1* signal was related to lower *SOST* mRNA levels in iliac crest bone biopsies, particularly in Affymetrix chip analyses, whereas no association was observed for *B4GALNT3* or *TNFRSF11B* (Supplementary Table 15).

Methylation QTLs lookups for sclerostin signals

To evaluate if our top association signals have the potential to influence DNA methylation, we cross-referenced the sclerostin SNPs with *cis*-methylation data from blood cells obtained at five different time points (ALSPAC children at Birth, Childhood and Adolescence; ALSPAC mothers during Pregnancy and at Middle age (30)). We found that our top hit rs215226, within *B4GALNT3*, was consistently associated with cg20907806 and cg26388816 across four time points (Supplementary Table 16). These two CpG sites are located in a CpG island that overlapped with one of the four ATAC-seq peaks within the *B4GALNT3* region

(Supplementary Figure 7, upper plot). The other potential signal near *TNFRSF11B*, rs1485303, was associated with cg13268132 and cg17171407 at all five time points.

B4galnt3 mRNA expression pattern

In murine gene expression studies, *B4galnt3* mRNA was expressed at highest levels in kidney, with relatively high levels of expression also observed in bone, particularly cortical bone (Figure 3A). *B4galnt3* mRNA was subsequently found to be expressed at relatively high levels in osteoblast cultures derived from neonatal mouse calvariae. The expression in osteoblast cultures was similar after 2 and 4 days of culture in osteogenic media (Figure 3B). After 7 days culture there was a suggestive increase in *B4galnt3* expression. No expression was detected in *in vitro* cultured mouse bone marrow macrophages or osteoclasts (Figure 3B).

DISCUSSION

Having performed a GWAS meta-analysis of serum sclerostin, we identified two genome-wide significant loci (*B4GALNT3* and *GALNT1*), and a further locus close to genome wide significance (*TNFRSF11B*). Together, common HapMap3 variants explained 16% of the variance of serum sclerostin. By using rs215226 in *B4GALNT3* and rs7241221 in *GALNT1* to examine causal relationships between serum sclerostin and BMD, we found evidence of an inverse relationship between sclerostin and BMD, and a positive relationship with fracture risk, in line with randomized control trial findings that the sclerostin inhibitor romosozumab increases BMD and reduces fracture risk (2)(3). Moreover, association signals with sclerostin at these two loci colocalized with those for eBMD, consistent with the possibility that genetic variation in *B4GALNT3* and *GALNT1* alters BMD via changes in serum sclerostin. Although our analyses were primarily intended to identify loci associated with serum sclerostin, there is some evidence to suggest that rs215224 was responsible for the underlying genetic signal at the *B4GALNT3* locus. This SNP is in perfect LD with our top *B4GALNT3* hit, rs215226. Rs215224 shows strong evidence of alteration of transcriptional activity from RegulomeDB, supported by the finding that this SNP falls within an ATAC-seq site of E15.5 mouse femurs. That said, though rs215224was also associated with differential methylation at two distinct CPG sites within *B4GALNT3*, one of which coincided with an ATAC-seq site, these were at distinct locations within the gene.

The *B4GALNT3* locus that we observed to be strongly related to serum sclerostin expresses a Golgi enzyme, beta-1,4-N-acetyl-galactosaminyltransferase, which transfers a GalNac residue to a nonreducing terminal GlcNAc-β, producing the disaccharide structure LacdiNAc. *B4GALNT3* has previously been reported to be expressed in multiple human tissues, including arterial, gastrointestinal tract and testis (31). In the present study, in mice, *B4GALNT3* mRNA was expressed at highest levels in kidney and cortical bone. This finding is consistent with high levels of *B4GALNT3* mRNA expression in renal tissue from human fetal samples in the NIH Roadmap Epigenomics Mapping Consortium (see https://www.ebi.ac.uk/gxa/experiments/, data from http://www.roadmapepigenomics.org/data/). The *B4GALNT3* locus we identified showed strong *cis*-regulatory activity in eQTL studies in arterial tissue, which was confirmed by the colocalization analysis. The effect allele associated with higher sclerostin levels was associated with considerably greater *B4GALNT3* mRNA levels in arterial tissue, suggesting that B4GALNT3 acts to increase sclerostin levels.

Sclerostin is a glycoprotein which, like *B4GALNT3*, is also expressed at a number of sites outside the skeleton including arterial tissue (32). Whereas sclerostin protein is detected in multiple tissues, extra-skeletal sclerostin mRNA is mainly expressed in the kidney, reflecting renal tubular expression (www.proteinatlas.org), suggesting this may be the predominant extra-skeletal source of circulating sclerostin. It's tempting to speculate that sclerostin acts as a substrate for *B4GALNT3*, such that formation of a terminal LacdiNAc moiety protects sclerostin from degradation and clearance from the circulation (see Figure 4). This interpretation is analogous to the role of *GALNT3*, a Golgi enzyme which acts to O-glycosylate another osteocyte-derived protein, FGF23, protecting it from degradation (33). Given our finding that B4GALNT3 is expressed at high levels in the kidney, a major source of extra-skeletal sclerostin, the kidney may represent the principle source of glycosylated sclerostin. To the extent that activity of renal sclerostin glycosylation influences BMD via changes in circulating sclerostin levels, rather than the latter simply reflecting 'spill over' from sclerostin within the bone micro environment, a two-way exchange may exist whereby perturbations in circulating sclerostin levels alter concentrations within bone. The *GALNT1* locus, which was also associated with serum sclerostin, expresses an enzyme that initiates O-glycosylation (34), and may act similarly to alter sclerostin levels by reducing sclerostin clearance.

In addition, we found that *B4GALNT3* is expressed at relatively high levels in bone, particularly cortical bone, where sclerostin is also preferentially expressed, reflecting its production by osteocytes. Specifically, *B4GALNT3* mRNA expression was detected in osteoblast cultures derived from mouse calvariae, but not in bone marrow macrophage cultures induced to form osteoclasts. Further studies are required to establish whether B4GALNT3 is expressed in osteocytes as well as osteoblasts. However, to the extent that B4GALNT3 and sclerostin expression overlap within bone, theoretically, B4GALNT3-dependent glycosylation might influence local sclerostin activity in a variety of ways, including altered production. Although genetic variation in *B4GALNT3* might conceivably influence circulating sclerostin via a primary action in bone, against this suggestion, there was little evidence of *B4GALNT3 cis*-regulatory activity in osteoblasts and bone tissue. Furthermore, the *B4GALNT3* SNP did not appear to act as a trans-eQTL signal for *SOST* in bone. However, eQTL studies in bone had considerably less power than those in other tissues analysed (285 and 78 individuals for tibial artery and bone biopsy studies respectively).

Genetic variation within the *SOST* gene appeared to have relatively weak associations with serum sclerostin, including *SOST* SNPs previously reported to be associated with BMD or hip fracture. This suggests that previously identified *SOST* SNPs influence BMD and hip fracture by altering local sclerostin activity in bone, independently of circulating sclerostin levels. That said, further studies with a larger sample size are needed to establish the contribution of genetic variation within the *SOST* locus to serum sclerostin. In terms of other genetic influences on serum sclerostin, the association between *TNFRSF11B* and serum sclerostin was just below our threshold. The latter contains a well-established BMD locus (13), and the protein product, OPG, plays a major role in regulating bone resorption (35). However, against the suggestion that altered OPG production mediates this genetic association, eQTL studies in heart tissue revealed that rs1485303 (the most strongly associated SNP at this locus) is strongly associated with expression of the adjacent gene, *COLEC10*.

Whereas MR analyses using *B4GLANT3* and *GALNT1* as genetic instruments supported a causal influence of higher sclerostin levels in reducing BMD, bidirectional MR analysis suggested that if anything, higher BMD leads to greater sclerostin levels. This apparent positive influence of BMD on sclerostin levels is in line with previous reports of elevated sclerostin levels in individuals with extreme elevations in BMD (36), and of positive associations between serum sclerostin levels and lumbar spine and femoral neck BMD in postmenopausal women (29). One explanation for this latter relationship is that individuals with higher BMD have a relatively large amount of bone tissue, and therefore, produce more sclerostin as result of having greater numbers of osteocytes. Additionally, these causal relationships may represent components of a regulatory feedback pathway, such that greater bone formation leading to increased BMD stimulates sclerostin production, which then feed backs to reduce bone formation and hence limit BMD gains.

Strengths and weaknesses

This study represents the first GWAS of serum sclerostin. We identified two loci, and one further suggestive locus, which were previously unknown to be related to serum sclerostin, including *B4GALNT3*, encoding a galactosaminyl transferase, which had a relatively strong association for a common variant (i.e. 0.2SD change in serum sclerostin per allele). In terms of weaknesses, the total study sample of around 11,000 was relatively small. In addition,

different methods were used to measure sclerostin in the participating cohorts; as well as different ELISAs, the MANOLIS cohort used the OLINK proteomics platform. Nonetheless, similar genetic associations were observed across all four cohorts, suggesting different sclerostin measurement methods are unlikely to have importantly impacted on our results.

Conclusions

Having performed a GWAS meta-analysis for serum sclerostin, we identified two genome wide significant loci encoding glycosylation enzymes, namely *B4GALNT3* and *GALNT1*. Genetic association signals for sclerostin at both loci co-localised with BMD, raising the possibility that variation in sclerostin glycosylation represents a hitherto unrecognised determinant of osteoporosis risk. Given the interest in sclerostin as a target for new osteoporosis treatments (2)(3), and as a genetic basis for skeletal dysplasia (37)(38), understanding the contribution of glycosylation to sclerostin activity may yield new opportunities for medical application.

ONLINE METHODS

The Avon Longitudinal Study of Parents and Children (ALSPAC)

Cohort details ALSPAC is a prospective birth cohort which recruited pregnant women with expected delivery dates between April 1991 and December 1992 from Bristol UK. The initial number of pregnancies enrolled is 14,541 (for these at least one questionnaire has been returned or a "Children in Focus" clinic had been attended by 19/07/1999). Of these initial pregnancies, there was a total of 14,676 foetuses, resulting in 14,062 live births and 13,988 children who were alive at 1 year of age. Detailed information on health and development of children and their parents were collected from regular clinic visits and completion of questionnaires (39)(40). Ethical approval was obtained from the ALSPAC Law and Ethics Committee and the Local Ethics Committees. Please note that the study website contains details of all the data that is available through a fully searchable data dictionary (http://www.bristol.ac.uk/alspac/researchers/our-data/).

Sclerostin measurements Sclerostin was measured in heparin plasma from 9312 individuals (both children and mothers) in ALSPAC using Biomedica Human Sclerostin ELISA (BI-20492, Biomedica Medizinprodukte, Vienna, Austria) kit. According to the manufacture's protocol, the standard range for the array kit was 0 – 240 pmol/l and the lower detection limit was 3.2 pmol/l. Each kit was run with an internal quality control. All samples were run in duplicate and if the sclerostin measurement differed more than 20% between the duplicates, we removed the individual from further analysis. Outliers four SDs away from the mean value were excluded. After these exclusions, 8772 individuals with linked genetic and demographic data were available for analysis (see Table 1).

Genotyping A total of 10584 participants were genotyped using the Illumina HumanHap550 quad genome-wide SNP genotyping platform. Data were imputed to the Haplotype Reference Consortium (HRC) reference panel v1.0. Quality control assessment were described in Supporting Information. After quality control assessment and imputation, the data set consisted of 8365 individuals, 7,052,184 SNPs available for analysis. 7292 of the 8772 individuals with both genotype and valid sclerostin measures were available for the GWAS analysis.

Die Deutsche Diabetes Dialyse Studie (4D)

Cohort details The 4D study was a prospective randomized controlled trial including patients with type 2 diabetes mellitus who had been treated by hemodialysis for less than 2 years (41). Between March 1998 and October 2002, 1255 patients were recruited in 178 dialysis centres in Germany. Patients were randomly assigned to double-blinded treatment with either 20 mg of atorvastatin (n = 619) or placebo (n = 636) once daily and were followed up until the date of death, censoring, or end of the study in March 2004. The primary end point of the 4D study was defined as a composite of death due to cardiac causes, stroke, and myocardial infarction, whichever occurred first. 4D study end points were centrally adjudicated by 3 members of the endpoints committee blinded to study treatment and according to predefined criteria. The study was approved by the medical ethics committees, and written informed consent was obtained from all participants.

Sclerostin measurements Sclerostin was assessed in serum from 1187 study participants by the TECO® Sclerostin EIA Kit, which is a 96-well immuno-capture ELISA. All measurements were done within one batch by personnel blinded to the study results. Serum samples were incubated with a biotinylated polyclonal antibody as well as with a horseradish peroxidase-labelled secondary monoclonal antibody that specifically recognizes human sclerostin. According to the instruction manual for human sclerostin HS EIA kit provided by TECOmedical (TECOmedical AG, Sissach, Switzerland), the lower limit of detection is 0.008 ng/mL and the upper limit of quantification is 3.34 ng/ml. Each kit used for 4D sclerostin measurements was accompanied by internal quality controls revealing a coefficient of variation = 4.4% for low sclerostin controls and a coefficient of variation = 2.7% for high sclerostin controls.

Genotyping A total of 1255 study participants were genotyped using the Genome-Wide Human SNP Array 6.0 from Affymetrix. Data were imputed to the Haplotype Reference Consortium (HRC) reference panel v1.0. After quality control assessment and imputation, the data set consisted of 1100 individuals. 1041 individuals with genotype and valid sclerostin measures were available for the GWAS analysis.

GOOD Cohort

Cohort details The Gothenburg Osteoporosis and Obesity Determinants (GOOD) study was initiated to determine both environmental and genetic factors involved in the regulation of bone and fat mass (42). Male study subjects were randomly identified in the greater

Gothenburg area in Sweden using national population registers, contacted by telephone, and invited to participate. To be enrolled in the GOOD study, subjects had to be between 18 and 20 years of age. There were no other exclusion criteria, and 49% of the study candidates agreed to participate (n = 1068). The study was approved by the ethics committee at the University of Gothenburg. Written and oral informed consent was obtained from all study participants.

Sclerostin measurements At the baseline visit, blood samples were drawn, serum was separated, and within 1 hour, the samples were frozen and stored at −80°C. During transport, the samples were kept on dry ice, and they were not thawed until ready for analysis at TECO Medical, Bünde, Germany. Serum sclerostin was analysed using TECO Sclerostin EIA Kit (TE1023-HS, TECOmedical AG, Sissach, Switzerland) with a sensitivity of 0,13 pg/ml and an intra-assay precision with CV 9.6% at 0,45 pg/ml and CV 4.1% at 1.34 pg/ml.

Genotyping Genotyping was performed using the Illumina HumanHap610 Quad arrays and genotypes were called using the BeadStudio calling algorithm. Genotypes from 938 individuals passed the sample quality control criteria [exclusion criteria: sample call rate < 97.5%, gender discrepancy with genetic data from X-linked markers, excess autosomal heterozygosity > 0.33 ~ FDR < 0.1%, duplicates and/or first-degree relatives identified using IBS probabilities (> 97%), ethnic outliers (3 SD away from the population mean) using multi-dimensional scaling analysis with four principal components]. Across 22 duplicate samples, genotype concordance exceeded 99.9%. Data were first pre-phased without a reference panel, using SHAPEIT2, and then imputed to the Haplotype Reference Consortium reference panel, using Sanger Imputation Service. The HRC.r1 release consists of 64,940 haplotypes and a total of 40,405,505 variants of predominantly European ancestry. 935 individuals with valid sclerostin measurements and imputed dosage in 8153657 variants were used in the GWAS analysis.

MANOLIS Cohort

Cohort details the HELIC-MANOLIS (Minoan isolates) collection comprises individuals from the mountainous Mylopotamos villages, including Anogia, Zoniana, Livadia and Gonies (estimated population size of 6,000 in total) on the Greek island of Crete. It is one of the two cohorts composing the Hellenic Isolated Cohorts study (HELIC - http://www.helic.org). The specific population genetics (43) and dietary and lifestyle habits (44) of this cohort have been

previously studied in the literature. The HELIC collections include blood for DNA extraction, laboratory-based haematological and biochemical measurements, and interview-based questionnaire data. The study was approved by the Harokopio University Bioethics Committee, and informed consent was obtained from human subjects.

Sclerostin measurements 92 proteins were assayed using the OLINK (www.olink.com) platform in 1,407 samples from the MANOLIS cohort as part of the Metabolism protein panel, where Sclerostin is present under the name SOST. Raw sclerostin normalised protein expression (NPX, https://www.olink.com/question/what-is-npx/) values from the OLINK platform were adjusted for sex, age, age squared, season of collection and total protein levels across 273 proteins in the CVDII, CVDIII and Metabolism panels, and the residuals were standardised.

Genotyping 1,482 samples were sequenced at 22x depth using Illumina HiSeq X Ten. Variant calling was performed using the GATK (45) best practices and association was performed using GEMMA (46), using an empirical relatedness matrix calculated on a LD-pruned set of common variants (MAF>5%) filtered for Hardy-Weinberg Equilibrium p<1x10-5. At the association stage, variants were not filtered for Hardy-Weinberg Equilibrium. Full details of the sequencing, variant calling and association protocol have been previously described (47). After sequencing and phenotype QC, 1,316 samples had both genotype and phenotype data available in the MANOLIS cohort.

GWAS Meta-analysis of sclerostin

Sclerostin measures in the four cohorts were standardized to SD units. Each cohort ran a GWAS across all imputed or sequenced variants. Age, sex and the first 10 principal components (PCs) were included as covariates in all models. Linear mixed models BOLT-LMM and GEMMA were applied to ALSPAC and MONOLIS cohort, respectively, to adjust for cryptic population structure and relatedness. We standardized the genomic coordinates to be reported on the NCBI build 37 (hg19), and alleles on the forward strand. Summary level quality control was conducted for Europeans only in EasyQC (48). Meta-analysis (using a fixed-effects model implemented in EasyQC) was restricted to variants common to all four studies (n=5,245,208 variants), MAF >1%, and high imputation quality score (Rsq >0.8 for variants imputed in MACH (49) and info >0.8 for variants imputed in IMPUTE (50)). $P < 5\times10^{-8}$ in the meta-analysis was used to define genome-wide significant associations. Each

locus is represented in the corresponding results table by the variant with the strongest evidence for association. A random effects model meta-analysis was also conducted using GWAMA version 2.2.2 (51). Heterogeneity was assessed using the I2 statistic and Cochrane's Q test.

Conditional analysis

To detect multiple independent association signals at each of the genome-wide significant sclerostin loci, we carried out an approximate conditional and joint genome-wide association analysis using the software package GCTA-COJO (52). SNPs with high collinearity (Correlation R2 > 0.9) were ignored, and those situated more than 10 Mb away were assumed to be in complete linkage equilibrium. A reference sample of 8890 unrelated individuals of from ALSPAC mothers was used to model patterns of LD between variants. The reference genotyping data set consisted of the same 5 million variants assessed in our GWAS. Conditionally independent variants that reached GWAS significance were annotated to the physically closest gene with the Hg19 Gene range list available in dbSNP (https://www.ncbi.nlm.nih.gov/SNP/).

Estimation of SNP heritability using Linkage disequilibrium (LD) score regression

To estimate the amount of genomic inflation in the data due to residual population stratification, cryptic relatedness and other latent sources of bias, we used LD score regression (11). LD scores were calculated for all high-quality SNPs (i.e., INFO score > 0.9 and MAF > 0.1%) from the meta-analysis data set consisting of 10,584 individuals from the 4 cohorts. We further quantified the overall SNP-based heritability's with LD score regression using a subset of 1.2 million HapMap SNPs.

Genetic analysis between sclerostin and bone phenotypes

Estimation of genetic correlations using LD Hub

To estimate the genetic correlation between sclerostin and bone phenotypes related to osteoporosis, we used a recent method based on LD score regression as implemented in the online web utility LD Hub (16). This method uses the cross-products of summary test statistics from two GWASs and regresses them against a measure of how much variation each SNP tags (its LD score). Variants with high LD scores are more likely to contain more true signals and thus provide a greater chance of overlap with genuine signals between GWASs. The LD score regression method uses summary statistics from the GWAS meta-

analysis of sclerostin and the bone phenotypes, calculates the cross-product of test statistics at each SNP, and then regresses the cross-product on the LD score.

Mendelian randomization of sclerostin on bone phenotypes

We undertook two sample MR (53) to evaluate evidence of a causal relationship between sclerostin measured in plasma and bone phenotypes. In this initial analysis, sclerostin was treated as the exposure and bone traits as the outcomes, using sclerostin associated SNPs as the instrumental variables. The multiple testing p-value threshold was calculated as p = 0.05 divided by the derived number of independent tests. We used the random effect inverse variance weighted (IVW) (53) and Wald ratio (54) methods to obtain MR effect estimates. Heterogeneity analysis of the instruments were conducted using Cochran Q test. Results were plotted as forest plots using code derived from the ggplot2 package in R (55). All MR analysis were conducted using the MR-Base TwoSampleMR R package (github.com/MRCIEU/TwoSampleMR, (56).

Genetic colocalization analysis between sclerostin and bone phenotypes

We used a stringent Bayesian model (coloc) to estimate the posterior probability (PP) of each genomic locus containing a single variant affecting both serum sclerostin level and bone phenotypes (57). A lack of evidence (i.e. PP < 80%) in this analysis would suggest that one of the causal variants for protein is simply in linkage disequilibrium (LD) with the putative causal variant for the trait (thus introducing genomic confounding into the association between sclerostin level and bone phenotypes). We treated colocalised findings (PP>=80%) as “Colocalised”, and other findings that did not pass colocalization as “Not colocalised”.

Bidirectional MR

To investigate the possibility that BMD causally affects levels of serum sclerostin, we used summary results data from 49 conditionally independent autosomal variants reported in a femoral neck BMD GWAS using 32,744 GEFOS individuals (17). We looked up these variants in summary results GWAS data on sclerostin from our meta-analysis and found 32 instruments for femoral neck BMD and 27 instruments for lumbar spine BMD. When applying bidirectional MR, we assume that SNPs used to proxy BMD exert their primary association on BMD, and that any correlation with sclerostin levels is a consequence of a causal effect of BMD on sclerostin. However, if in reality sclerostin levels exert a causal effect on BMD, then it is possible that some sclerostin SNPs might also reach genome-wide

significance in a large GWAS of BMD. These sclerostin SNPs could then mistakenly be used as instruments for BMD, when in fact they should be used as instruments for sclerostin levels. This was the case in the GEFOS and UKBB studies as some of the BMD associated SNPs were also strongly associated with sclerostin (i.e. at genome-wide levels of significance). We therefore applied MR Steiger filtering (20) as implemented in the TwoSampleMR R package (56) to test the causal direction of each BMD associated SNP on the hypothesized exposures (BMD) and outcome (sclerostin). We removed those sclerostin SNPs and performed inverse variance weighted (IVW) MR to identify the causal estimates of femoral neck and lumbar spine BMD on sclerostin. We further performed weighted median and MR-Egger regression methods that are more robust to the presence of genetic pleiotropy (which means BMD associated SNPs may influence sclerostin via additional pleiotropic paths that do not pass through BMD levels). We then performed pleitropy test using MR Egger intercept and heterogeneity test using Cochrane Q test. To identify outlier instruments of the exposures (FN-BMD and LS-BMD), we applied RadialMR R package (21)(22) to estimate the individual contribution of each instruments to overall heterogeneity (in another word, the Cochrane Q of each SNP with 1 degree of freedom) and used the corresponding Cochrane p-value to detect outliers ($P<0.05$). As a sensitivity analysis, we removed outliers and conducted the bidirectional MR again. All bidirectional MR were conducted using the TwoSampleMR (56) package.

Functional annotation

Predicted regulatory elements of the top association signals

For each locus associated with sclerostin, we identified all SNPs with high linkage disequilibrium (LD) from the top signal (LD $r^2>0.8$) and identify their DNA features and regulatory elements in non-coding regions of the human genome using Regulomedb v1.1 (http://www.regulomedb.org/) (23).

ATAC-seq lookup in the top association regions

The Assay for Transposase Accessible Chromatin with high-throughput sequencing (ATAC-seq) is a method for mapping chromatin accessibility genome-wide (25). We intersected the sclerostin associated SNPs (or proxy SNPs with LD $r^2 > 0.8$) with ATAC-seq data generated from the proximal and distal femur of an E15.5 mouse (24) (25) lifted over to the orthologous positions in human genome build hg19).

Gene expression quantitative trait loci (eQTLs) lookups for sclerostin signals

We investigated whether the SNPs influencing serum sclerostin level were driven by cis-acting effects on transcription by evaluating the overlap between the sclerostin associated SNPs and eQTLs within 500kb of the gene identified, using data derived from all tissue types from the GTEx consortium v7 (27). Evidence of eQTL association was defined as $P < 1x10^{-4}$ and evidence of overlap of signal was defined as high LD ($r2 \geq 0.8$) between eQTL and sclerostin associated SNPs in the region. Where eQTLs overlapped with sclerostin associated SNPs, we used the colocalization analysis to estimate the posterior probability (PP) of each genomic locus containing a single variant affecting both serum sclerostin level and gene expression level in different tissues. Equivalent analyses were performed in human primary osteoblast cells (28), and cells derived from iliac crest bone from 78 postmenopausal women (29). In the latter, mRNA was quantified both by Affymetrix RNA chip and RNA-seq. RNA-Seq analyses were evaluating using a pipeline previously described (58) and publicly available (https://github.com/molgenis/systemsgenetics/wiki/eQTL-mapping-analysis-cookbook-for-RNA-seq-data). Briefly, gene expression data was TMM (trimmed mean of M values), normalized [18] and log2-transformed. Then, expression of each gene was centred and scaled. To reduce the effect of non-genetic sources of variability, we applied principal component analysis on the sample correlation matrix and the first five components were used as covariates. cis-eQTL analysis was performed on transcript-SNP combinations for which the distance from the centre of the transcript to the genomic location of the SNP was ≤250 kb, whereas eQTLs with a distance greater than 5 Mb were defined as trans-eQTLs. Associations were tested by non-parametric Spearman's rank correlation and a threshold of false discovery rate (FDR<0.05) applied. Analyses were adjusted for age, BMI and four genomic principle components.

Methylation quantitative trait loci (mQTLs) lookups for sclerostin signals

We also investigated whether the SNPs influencing serum sclerostin level were mediated by cis-acting effects on DNA methylation by evaluating the overlap between the sclerostin associated SNPs and mQTLs within 500kb of the gene identified, using data measured in blood cells. We queried data from mQTLdb, which contained mQTL information at 5 different time points, ALSPAC children at Birth, Childhood and Adolescence and ALSPAC mothers during Pregnancy and at Middle age. This data is from the ARIES resource (30). Evidence of mQTL association was defined as $P < 1x10^{-4}$ and evidence of overlap of signal

was defined as high LD ($r2 \geq 0.8$) between mQTL and sclerostin associated SNPs in the region.

Expression of *B4galnt3*

B4galnt3 mRNA expression was analysed in a range of tissues, including different bone compartments as well as in *in vitro* cultured macrophages, osteoblasts and osteoclasts. Tissues were dissected from 22 weeks old female C57Bl/6 mice. Total RNA was prepared using TriZol Reagent (Life Technologies) followed by RNeasy Mini Kit (Qiagen). The RNA was reverse-transcribed into cDNA, and real-time PCR analysis was performed using a predesigned real-time PCR assay for *B4galnt3* (Mm01189804_m1) and the StepOnePlus Real-Time PCR system (Applied Biosystems). The mRNA abundance was adjusted for the expression of 18S. Primary calvarial osteoblasts were isolated from 3-5 days old C57Bl/6 mice by sequential digestion as described previously (59) Cells were cultured in complete α-MEM medium (MEM alpha medium (Gibco, 22561-021)) supplemented with 10% heat-inactivated FBS (Sigma, F7524), 2 mM GlutaMAX (Gibco, 35050-038), 50 µg/ml gentamicin (Gibco, 15750-037), 100 U/ml penicillin and 100 µg/ml streptomycin (Gibco, 15140-148) for 4-6 days before subculture in 48-well plates at 40,000 cells cm^{-2} and induction of osteogenic differentiation in complete α-MEM supplemented with 10 mM β-glycerophosphate disodium salt hydrate (BGP; Sigma, G9422) and 0.2 mM L-ascorbic acid 2-phosphate sesquimagnesium salt hydrate (Asc-2P; Sigma, A8960) for 2, 4 and 7 days. Bone marrow macrophages were isolated and amplified by culturing bone marrow cells from 8-12 weeks old C57Bl/6 in suspension culture discs (Corning Costar Ins., NY) in complete α-MEM with 30 ng/ml M-CSF (R&D, 416-ML-050) for two days. Thereafter, the adherent macrophages were detached, and spot seeded in 24-well plates (40,000 cells/well). Macrophages were cultured for additional 3 days in complete α-MEM with 30 ng/ml M-CSF before gene expression analysis. For osteoclast generation, macrophages were cultured in 30 ng/ml M-CSF and 4 ng/ml RANKL (R&D, 462-TEC) for 3 days. RNA was isolated from cell cultures after cell lysis in RLT buffer using RNeasy Micro Kit (Qiagen), and gene expression was analysed as above. Cell culture experiments were performed in quadruplicates and repeated twice with similar results.

FIGURE LEGENDS

Figure 1

Regional association plots and ENCODE annotation of the loci that reached or marginally reached genome-wide significance ($P < 5 \times 10^{-8}$) in the meta-analysis. The X-axis indicates the physical position of each SNP on the chromosome specified, whereas the Y-axis denotes the evidence of association shown as −log(P-value). A) the *B4GLANT3* region; 2) the *GALNT1* region and 3) the *TNFRSF11B* region.

Figure 2

Forest plot of putative causal relationship between serum sclerostin and bone phenotypes using Mendelian randomization. X-axis represents the causal estimates and 95% confidence intervals of SD change in BMD/eBMD and OR for fracture, per SD increase in sclerostin, as calculated by inverse variance weighted method. Y-axis lists the four bone phenotypes used in the MR analysis.

Figure 3

B4galnt3 expression in mice and in *in vitro* cultured osteoblasts and osteoclasts. A. *B4galnt3* mRNA tissue expression in adult female mice, presented as % of cortical bone ±SEM (n=6). B. *B4galnt3* mRNA expression in mouse calvarial osteoblasts cultured in osteogenic media for 2, 4 and 7 days (D). Mouse bone marrow macrophages cultured with M-CSF (M), or M-CSF+RANKL (M/RL) to induce osteoclasts differentiation. % of expression D2 ±SEM. ND = not detectable

Figure 4

Proposed exchange of sclerostin between skeletal and systemic compartments. Sclerostin, synthesized by osteocytes, is present within the bone micro-environment, but also exchanges with the systemic circulation, where it is produced by several extra-skeletal tissues including the kidney. Whereas locally produced sclerostin is largely responsible for actions of sclerostin on bone, factors which influence circulating levels may also play a role, including variation in activity of B4GALNT3, which we propose protects sclerostin from degradation through generation of a terminal LacdiNAc.

ACKNOWLEDGEMENTS

We are extremely grateful to all the families who took part in the ALSPAC study, the midwives for their help in recruiting them, and the whole ALSPAC team, which includes interviewers, computer and laboratory technicians, clerical workers, research scientists, volunteers, managers, receptionists and nurses. ALSPAC data collection was supported by the Wellcome Trust (grants WT092830M; WT088806; WT102215/2/13/2), UK Medical Research Council (G1001357), and University of Bristol. The UK Medical Research Council and the Wellcome Trust (ref: 102215/2/13/2) and the University of Bristol provide core support for ALSPAC. GDS works in the Medical Research Council Integrative Epidemiology Unit at the University of Bristol MC_UU_00011/1.

AG and EZ are supported by Wellcome (098051). CD and CW were supported by the Federal Ministry of Education and Research of the Federal Republic of Germany (BMBF 01EO1504). ML has received lecture or consulting fees from Amgen, Lilly, Meda, UCB Pharma, Renapharma, Radius Health and Consilient Health.

TDC was supported by NSF grant (BCS-1518596). EG was supported by a CIHR Foundation Grant (FDN-148381). KMG and SR were supported by the South East Norway Health Authority under Grant number 52009/8029; the 6th EU framework program under Grant number LSHM-CT-2003-502941; Oslo University Hospital, Ullevaal under Grant number 52009/8029; Lovisenberg Diaconal Hospital. For RNA-Seq analyses we thank Joost Verlouw, Jeroen van Rooij and Masa Zrimšek for their help in the creation, managing and quality control of the RNAseq of data cells derived from iliac crest bone implementing and posterior implementation of the eQTL analysis pipeline. CM-G was supported by the Netherlands Organization for Health Research and Development (ZonMw VIDI 016.136.367).

REFERENCES

1. Galea GL, Lanyon LE, Price JS. Sclerostin's role in bone's adaptive response to mechanical loading. Bone. 2017 Mar;96:38–44.

2. Cosman F, Crittenden DB, Adachi JD, Binkley N, Czerwinski E, Ferrari S, et al. Romosozumab Treatment in Postmenopausal Women with Osteoporosis. N Engl J Med. 2016 Oct 20;375(16):1532–43.

3. Saag KG, Petersen J, Grauer A. Romosozumab versus Alendronate and Fracture Risk in Women with Osteoporosis. N Engl J Med. 2018 Jan 11;378(2):195–6.

4. Drake MT, Khosla S. Hormonal and systemic regulation of sclerostin. Bone. 2017 Mar;96:8–17.

5. Behets GJ, Viaene L, Meijers B, Blocki F, Brandenburg VM, Verhulst A, et al. Circulating levels of sclerostin but not DKK1 associate with laboratory parameters of CKD-MBD. PLoS One. 2017 May 11;12(5):e0176411.

6. Novo-Rodríguez C, García-Fontana B, Luna-Del Castillo JDD, Andújar-Vera F, Ávila-Rubio V, García-Fontana C, et al. Circulating levels of sclerostin are associated with cardiovascular mortality. PLoS One. 2018 Jun 21;13(6):e0199504.

7. Wędrychowicz A, Sztefko K, Starzyk JB. Sclerostin and its significance for children and adolescents with type 1 diabetes mellitus (T1D). Bone [Internet]. 2018 Aug 15; Available from: http://dx.doi.org/10.1016/j.bone.2018.08.007

8. Napoli N, Strollo R, Defeudis G, Leto G, Moretti C, Zampetti S, et al. Serum Sclerostin and Bone Turnover in Latent Autoimmune Diabetes in Adults. J Clin Endocrinol Metab. 2018 May 1;103(5):1921–8.

9. Weivoda MM, Youssef SJ, Oursler MJ. Sclerostin expression and functions beyond the osteocyte. Bone. 2017 Mar;96:45–50.

10. Davey Smith G, Ebrahim S. 'Mendelian randomization': can genetic epidemiology contribute to understanding environmental determinants of disease? Int J Epidemiol. 2003;32(1):1–22.

11. Bulik-Sullivan BK, Loh P-R, Finucane HK, Ripke S, Yang J, Schizophrenia Working Group of the Psychiatric Genomics Consortium, et al. LD Score regression distinguishes confounding from polygenicity in genome-wide association studies. Nat Genet. 2015 Mar;47(3):291–5.

12. Kemp JP, Morris JA, Medina-Gomez C, Forgetta V, Warrington NM, Youlten SE, et al. Identification of 153 new loci associated with heel bone mineral density and functional involvement of GPC6 in osteoporosis. Nat Genet. 2017 Oct;49(10):1468–75.

13. Rivadeneira F, Styrkársdottir U, Estrada K, Halldórsson BV, Hsu Y-H, Richards JB, et al. Twenty bone-mineral-density loci identified by large-scale meta-analysis of genome-wide association studies. Nat Genet. 2009 Nov;41(11):1199–206.

14. Zheng H-F, Forgetta V, Hsu Y-H, Estrada K, Rosello-Diez A, Leo PJ, et al. Whole-genome sequencing identifies EN1 as a determinant of bone density and fracture. Nature. 2015 Oct 1;526(7571):112–7.

15. Trajanoska K, Morris JA, Oei L, Zheng H-F, Evans DM, Kiel DP, et al. Assessment of the genetic and clinical determinants of fracture risk: genome wide association and mendelian randomisation study. BMJ. 2018 Aug 29;362:k3225.

16. Zheng J, Erzurumluoglu AM, Elsworth BL, Kemp JP, Howe L, Haycock PC, et al. LD Hub: a centralized database and web interface to perform LD score regression that maximizes the potential of summary level GWAS data for SNP heritability and genetic correlation analysis. Bioinformatics. 2017 Jan 15;33(2):272–9.

17. Estrada K, Styrkarsdottir U, Evangelou E, Hsu Y-H, Duncan EL, Ntzani EE, et al. Genome-wide meta-analysis identifies 56 bone mineral density loci and reveals 14 loci associated with risk of fracture. Nat Genet. 2012 Apr 15;44(5):491–501.

18. Bowden J, Hemani G, Davey Smith G. Detecting individual and global horizontal pleiotropy in Mendelian randomization: a job for the humble heterogeneity statistic? Am J Epidemiol [Internet]. 2018 Sep 5; Available from: http://dx.doi.org/10.1093/aje/kwy185

19. Timpson NJ, Nordestgaard BG, Harbord RM, Zacho J, Frayling TM, Tybjærg-Hansen A, et al. C-reactive protein levels and body mass index: elucidating direction of causation through reciprocal Mendelian randomization. Int J Obes. 2011 Feb;35(2):300–8.

20. Hemani G, Tilling K, Davey Smith G. Orienting the causal relationship between imprecisely measured traits using GWAS summary data. PLoS Genet. 2017 Nov;13(11):e1007081.

21. Bowden J, Del Greco M F, Minelli C, Lawlor D, Sheehan N, Thompson J, et al. Improving the accuracy of two-sample summary data Mendelian randomization: moving beyond the NOME assumption [Internet]. 2017 [cited 2017 Oct 5]. Available from: https://www.biorxiv.org/content/early/2017/07/05/159442.abstract

22. Bowden J, Spiller W, Del-Greco F, Sheehan N, Thompson J, Minelli C, et al. Improving the visualisation, interpretation and analysis of two-sample summary data Mendelian randomization via the radial plot and radial regression [Internet]. 2017 [cited 2018 Oct 15]. Available from: https://www.biorxiv.org/content/early/2017/10/11/200378

23. Boyle AP, Hong EL, Hariharan M, Cheng Y, Schaub MA, Kasowski M, et al. Annotation of functional variation in personal genomes using RegulomeDB. Genome Res. 2012 Sep;22(9):1790–7.

24. Buenrostro JD, Giresi PG, Zaba LC, Chang HY, Greenleaf WJ. Transposition of native chromatin for fast and sensitive epigenomic profiling of open chromatin, DNA-binding proteins and nucleosome position. Nat Methods. 2013 Dec;10(12):1213–8.

25. Ou J, Liu H, Yu J, Kelliher MA, Castilla LH, Lawson ND, et al. ATACseqQC: a Bioconductor package for post-alignment quality assessment of ATAC-seq data. BMC Genomics. 2018 Mar 1;19(1):169.

26. Guo M, Liu Z, Willen J, Shaw CP, Richard D, Jagoda E, et al. Epigenetic profiling of growth plate chondrocytes sheds insight into regulatory genetic variation influencing height. Elife [Internet]. 2017 Dec 5;6. Available from: http://dx.doi.org/10.7554/eLife.29329

27. GTEx Consortium, Laboratory DA &Coordinating C (LDACC)—Analysis WG, Statistical Methods groups—Analysis Working Group, Enhancing GTEx (eGTEx) groups, NIH Common Fund, NIH/NCI, et al. Genetic effects on gene expression across human tissues. Nature. 2017 Oct 11;550(7675):204–13.

28. Grundberg E, Kwan T, Ge B, Lam KCL, Koka V, Kindmark A, et al. Population genomics in a disease targeted primary cell model. Genome Res. 2009 Nov;19(11):1942–52.

29. Reppe S, Noer A, Grimholt RM, Halldórsson BV, Medina-Gomez C, Gautvik VT, et al. Methylation of bone SOST, its mRNA, and serum sclerostin levels correlate strongly with fracture risk in postmenopausal women. J Bone Miner Res. 2015 Feb;30(2):249–56.

30. Gaunt TR, Shihab HA, Hemani G, Min JL, Woodward G, Lyttleton O, et al. Systematic identification of genetic influences on methylation across the human life course. Genome Biol. 2016 Mar 31;17:61.

31. Sato T, Gotoh M, Kiyohara K, Kameyama A, others. Molecular cloning and characterization of a novel human β1, 4-N-acetylgalactosaminyltransferase, β4GalNAc-T3, responsible for the synthesis of N, N …. Journal of Biological [Internet]. 2003; Available from: http://www.jbc.org/content/278/48/47534.short

32. Didangelos A, Yin X, Mandal K, Baumert M, Jahangiri M, Mayr M. Proteomics characterization of extracellular space components in the human aorta. Mol Cell Proteomics. 2010 Sep;9(9):2048–62.

33. Garringer HJ, Fisher C, Larsson TE, Davis SI, Koller DL, Cullen MJ, et al. The role of mutant UDP-N-acetyl-alpha-D-galactosamine-polypeptide N-acetylgalactosaminyltransferase 3 in regulating serum intact fibroblast growth factor 23 and matrix extracellular phosphoglycoprotein in heritable tumoral calcinosis. J Clin Endocrinol Metab. 2006 Oct;91(10):4037–42.

34. Bennett EP, Weghuis DO, Merkx G, van Kessel AG, Eiberg H, Clausen H. Genomic organization and chromosomal localization of three members of the UDP-N-acetylgalactosamine: polypeptide N-acetylgalactosaminyltransferase family. Glycobiology. 1998 Jun;8(6):547–55.

35. Suda T, Takahashi N, Udagawa N, Jimi E, Gillespie MT, Martin TJ. Modulation of osteoclast differentiation and function by the new members of the tumor necrosis factor receptor and ligand families. Endocr Rev. 1999 Jun;20(3):345–57.

36. Gregson CL, Poole KES, McCloskey EV, Duncan EL, Rittweger J, Fraser WD, et al. Elevated circulating Sclerostin concentrations in individuals with high bone mass, with and without LRP5 mutations. J Clin Endocrinol Metab. 2014 Aug;99(8):2897–907.

37. Balemans W, Ebeling M, Patel N, Van Hul E, Olson P, Dioszegi M, et al. Increased bone density in sclerosteosis is due to the deficiency of a novel secreted protein (SOST). Hum Mol Genet. 2001 Mar 1;10(5):537–43.

38. Brunkow ME, Gardner JC, Van Ness J, Paeper BW, Kovacevich BR, Proll S, et al. Bone dysplasia sclerosteosis results from loss of the SOST gene product, a novel cystine knot-containing protein. Am J Hum Genet. 2001 Mar;68(3):577–89.

39. Boyd A, Golding J, Macleod J, Lawlor DA, Fraser A, Henderson J, et al. Cohort Profile: the 'children of the 90s'--the index offspring of the Avon Longitudinal Study of Parents and Children. Int J Epidemiol. 2013 Feb;42(1):111–27.

40. Fraser A, Macdonald-Wallis C, Tilling K, Boyd A, Golding J, Davey Smith G, et al. Cohort Profile: the Avon Longitudinal Study of Parents and Children: ALSPAC mothers cohort. Int J Epidemiol. 2013 Feb;42(1):97–110.

41. Wanner C, Krane V, März W, Olschewski M, Asmus H-G, Krämer W, et al. Randomized controlled trial on the efficacy and safety of atorvastatin in patients with type 2 diabetes on hemodialysis (4D study): demographic and baseline characteristics. Kidney Blood Press Res. 2004 Aug 16;27(4):259–66.

42. Lorentzon M, Swanson C, Andersson N, Mellström D, Ohlsson C. Free testosterone is a positive, whereas free estradiol is a negative, predictor of cortical bone size in young Swedish men: the GOOD study. J Bone Miner Res. 2005 Aug;20(8):1334–41.

43. Panoutsopoulou K, Hatzikotoulas K, Xifara DK, Colonna V, Farmaki A-E, Ritchie GRS, et al. Genetic characterization of Greek population isolates reveals strong genetic drift at missense and trait-associated variants. Nat Commun. 2014 Nov 6;5:5345.

44. Farmaki A-E, Rayner NW, Matchan A, Spiliopoulou P, Gilly A, Kariakli V, et al. The mountainous Cretan dietary patterns and their relationship with cardiovascular risk factors: the Hellenic Isolated Cohorts MANOLIS study. Public Health Nutr. 2017 Apr;20(6):1063–74.

45. DePristo MA, Banks E, Poplin R, Garimella KV, Maguire JR, Hartl C, et al. A framework for variation discovery and genotyping using next-generation DNA sequencing data. Nat Genet. 2011 May;43(5):491–8.

46. Zhou X, Stephens M. Genome-wide efficient mixed-model analysis for association studies. Nat Genet. 2012 Jun 17;44(7):821–4.

47. Gilly A, Suveges D, Kuchenbaecker K, Pollard MO, Southam L, Hatzikotoulas K, et al. Cohort-wide deep whole genome sequencing and the allelic architecture of complex traits [Internet]. 2018 [cited 2018 Oct 25]. Available from: https://www.biorxiv.org/content/early/2018/03/16/283481

48. Winkler TW, Day FR, Croteau-Chonka DC, Wood AR, Locke AE, Mägi R, et al. Quality control and conduct of genome-wide association meta-analyses. Nat Protoc. 2014 May;9(5):1192–212.

49. Li Y, Willer CJ, Ding J, Scheet P, Abecasis GR. MaCH: using sequence and genotype data to estimate haplotypes and unobserved genotypes. Genet Epidemiol. 2010 Dec;34(8):816–34.

50. Howie B, Fuchsberger C, Stephens M, Marchini J, Abecasis GR. Fast and accurate genotype imputation in genome-wide association studies through pre-phasing. Nat Genet. 2012 Jul 22;44(8):955–9.

51. Mägi R, Morris AP. GWAMA: software for genome-wide association meta-analysis. BMC Bioinformatics. 2010 May 28;11:288.

52. Yang J, Ferreira T, Morris AP, Medland SE, Genetic Investigation of ANthropometric Traits (GIANT) Consortium, DIAbetes Genetics Replication And Meta-analysis (DIAGRAM) Consortium, et al. Conditional and joint multiple-SNP analysis of GWAS summary statistics identifies additional variants influencing complex traits. Nat Genet. 2012 Mar 18;44(4):369–75, S1-3.

53. Burgess S, Butterworth A, Thompson SG. Mendelian randomization analysis with multiple genetic variants using summarized data. Genet Epidemiol. 2013 Nov;37(7):658–65.

54. Lawlor DA, Harbord RM, Sterne JAC, Timpson N, Davey Smith G. Mendelian randomization: using genes as instruments for making causal inferences in epidemiology. Stat Med. 2008 Apr 15;27(8):1133–63.

55. Wickham H. ggplot2: Elegant Graphics for Data Analysis [Internet]. Springer; 2016. 260 p. Available from: https://market.android.com/details?id=book-XgFkDAAAQBAJ

56. Hemani G, Zheng J, Elsworth B, Wade KH, Haberland V, Baird D, et al. The MR-Base platform supports systematic causal inference across the human phenome. Elife [Internet]. 2018 May 30;7. Available from: http://dx.doi.org/10.7554/eLife.34408

57. Giambartolomei C, Vukcevic D, Schadt EE, Franke L, Hingorani AD, Wallace C, et al. Bayesian test for colocalisation between pairs of genetic association studies using summary statistics. PLoS Genet. 2014 May;10(5):e1004383.

58. Deelen P, Zhernakova DV, de Haan M, van der Sijde M, Bonder MJ, Karjalainen J, et al. Calling genotypes from public RNA-sequencing data enables identification of genetic variants that affect gene-expression levels. Genome Med. 2015 Mar 27;7(1):30.

59. Granholm S, Henning P, Lindholm C, Lerner UH. Osteoclast progenitor cells present in significant amounts in mouse calvarial osteoblast isolations and osteoclastogenesis increased by BMP-2. Bone. 2013 Jan;52(1):83–92.

Table 1. Study information of the cohorts involved in the sclerostin GWAS meta-analysis.

COHORT	N SCLEROSTIN	N FEMALE SCLEROSTIN	N GWAS	AGE (SD)	ETHNIC OR RACIAL GROUP	FAMILY STRUCTURE	FAMILY STRUCTURE ADJUSTMENT	ASSAY DETAILS
ALSPAC	8772	6371	7292	Children: 9.9 (0.3) Mothers: 48 (4.4)	European	Mothers and Children	BOLT-LMM	Biomedica Human Sclerostin ELISA
4D	1041	468	1041	66.3 (8.36)	European	Unrelated	No adjustment	TECO
MANOLIS	1316	729	1316	61 (19)	European	Isolated population	GEMMA	OLINK
GOOD	935	0	935	18.9(0.56)	European	Unrelated	No adjustment	TECO

Table 2. Meta-analysis results for loci that reached or marginally reached genome-wide significance ($P < 5 \times 10^{-8}$).

SNP	EA	OA	EAF	GENE	BETA	SE	P	Q	Q_P	I^2	N
rs215226	A	G	0.597	*B4GALNT3*	0.205	0.014	4.60E-49	13.430	0.0038	0.777	10584
rs7241221	G	A	0.772	*GALNT1*	0.109	0.017	4.40E-11	0.955	0.812	0	10584
rs1485303	G	A	0.568	*TNFRSF11B*	0.074	0.014	7.70E-08	6.416	0.093	0.532	10584

Note: EA (effect allele), OA (other allele), EAF (effect allele frequency), GENE (nearest gene to the sclerostin associated SNP), N (sample size of the GWAS meta-analysis); BETA (SD change in serum sclerostin per effect allele), SE (standard error) and P (p-value)) Heterogeneity test (Q (Cochrane's Q statistics), Q_P (Cochrane's Q P value), I^2 (I^2 statistics))

Figure 1

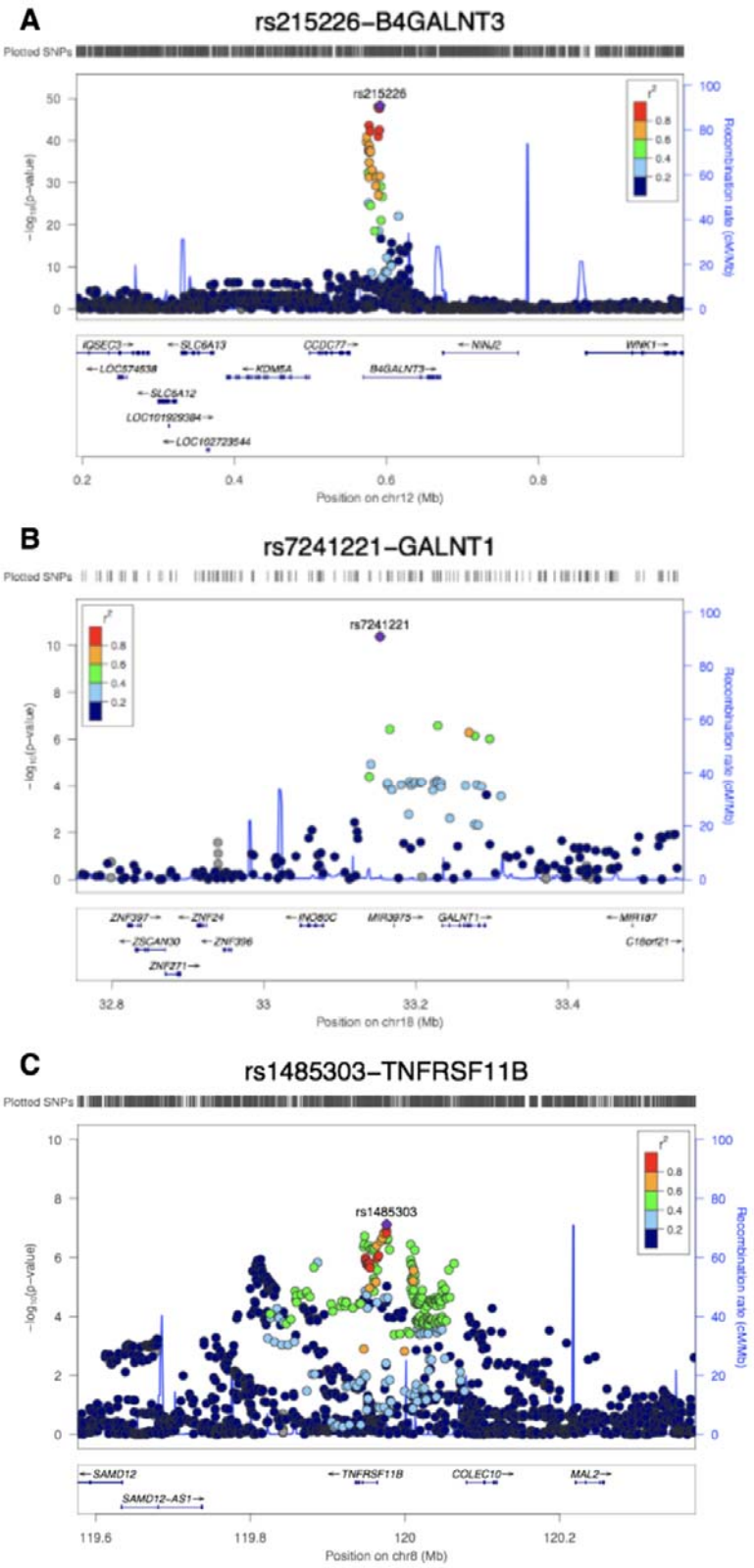

Figure 2

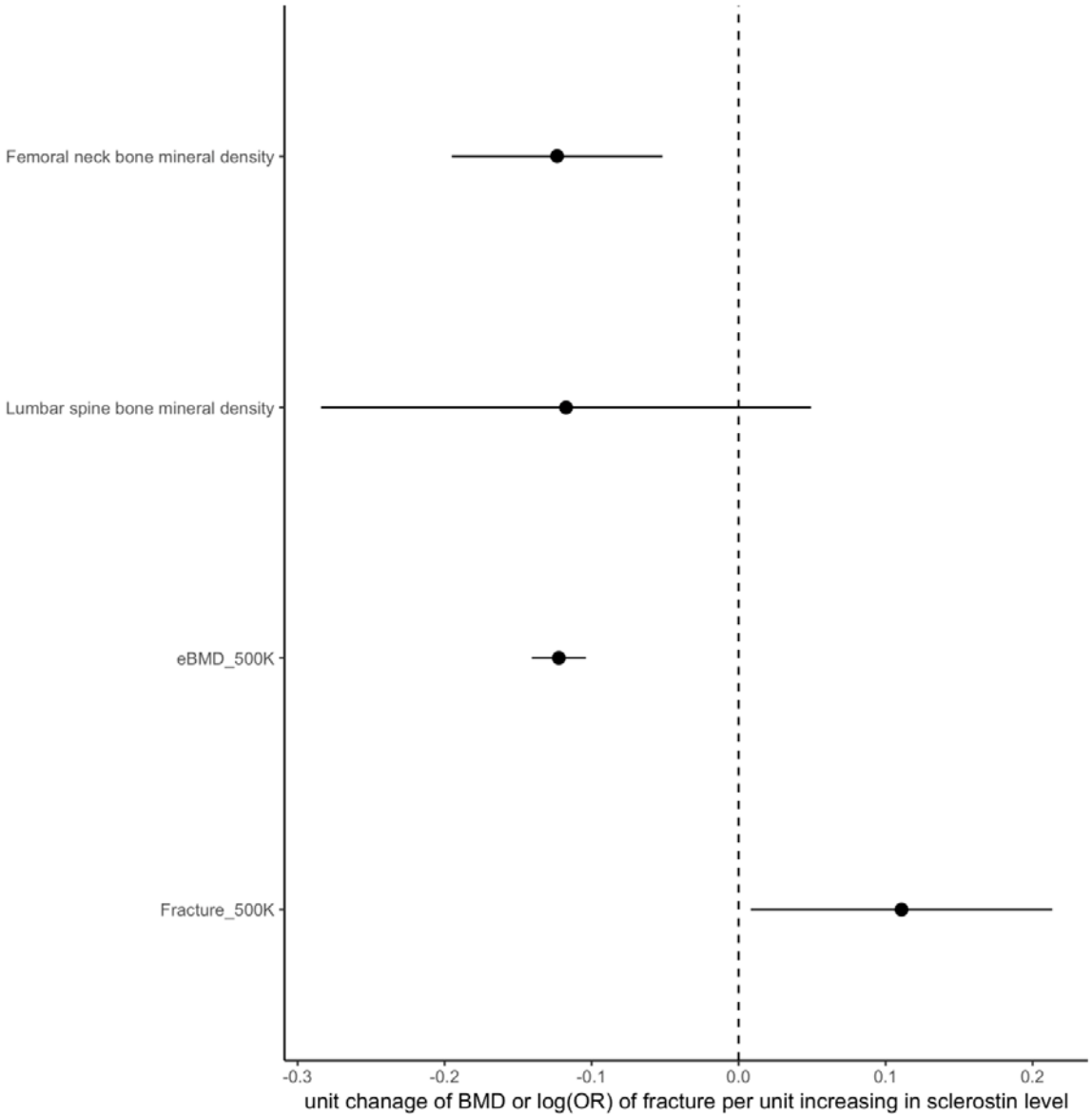

Figure 3

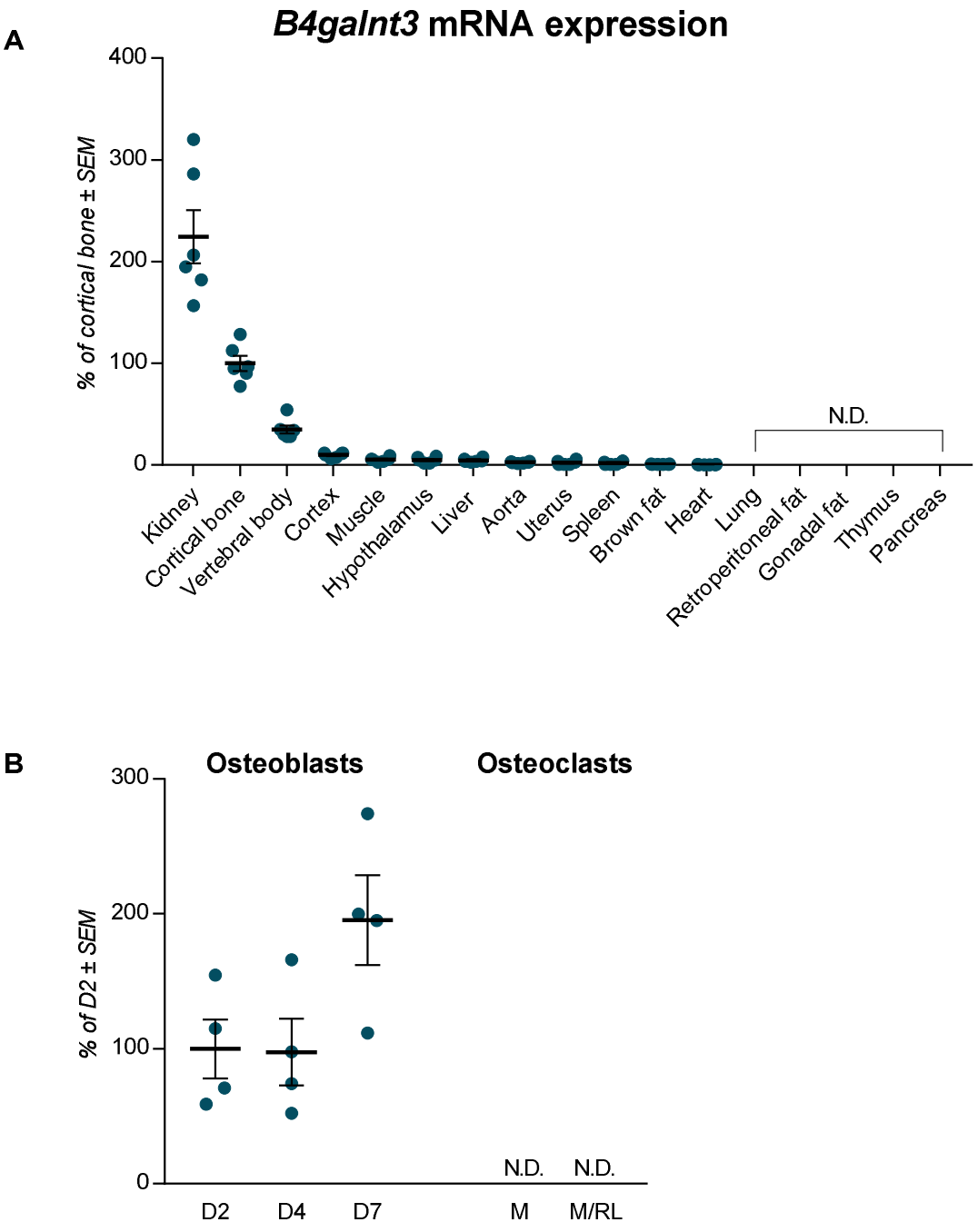

Figure 4

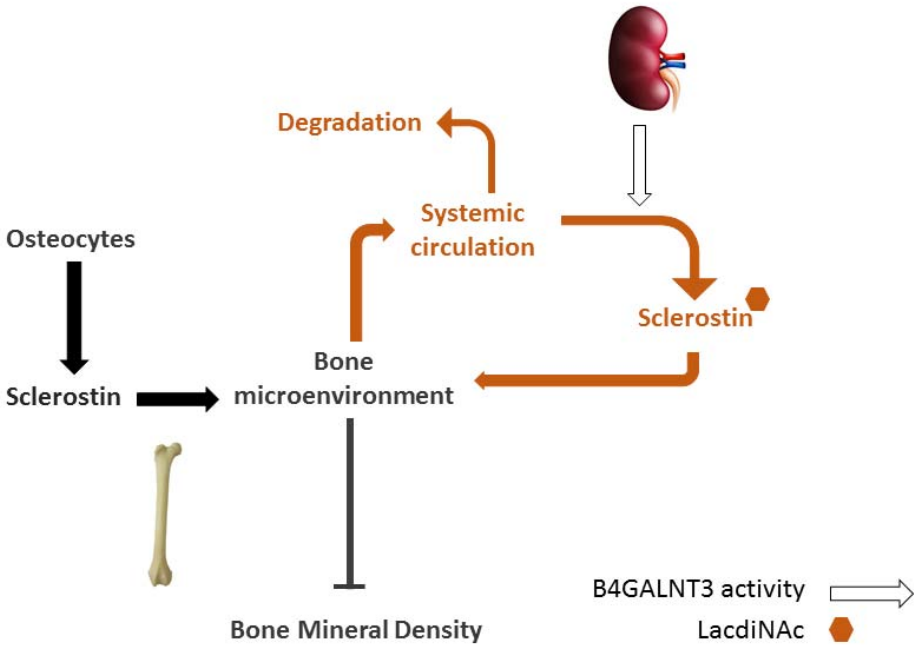

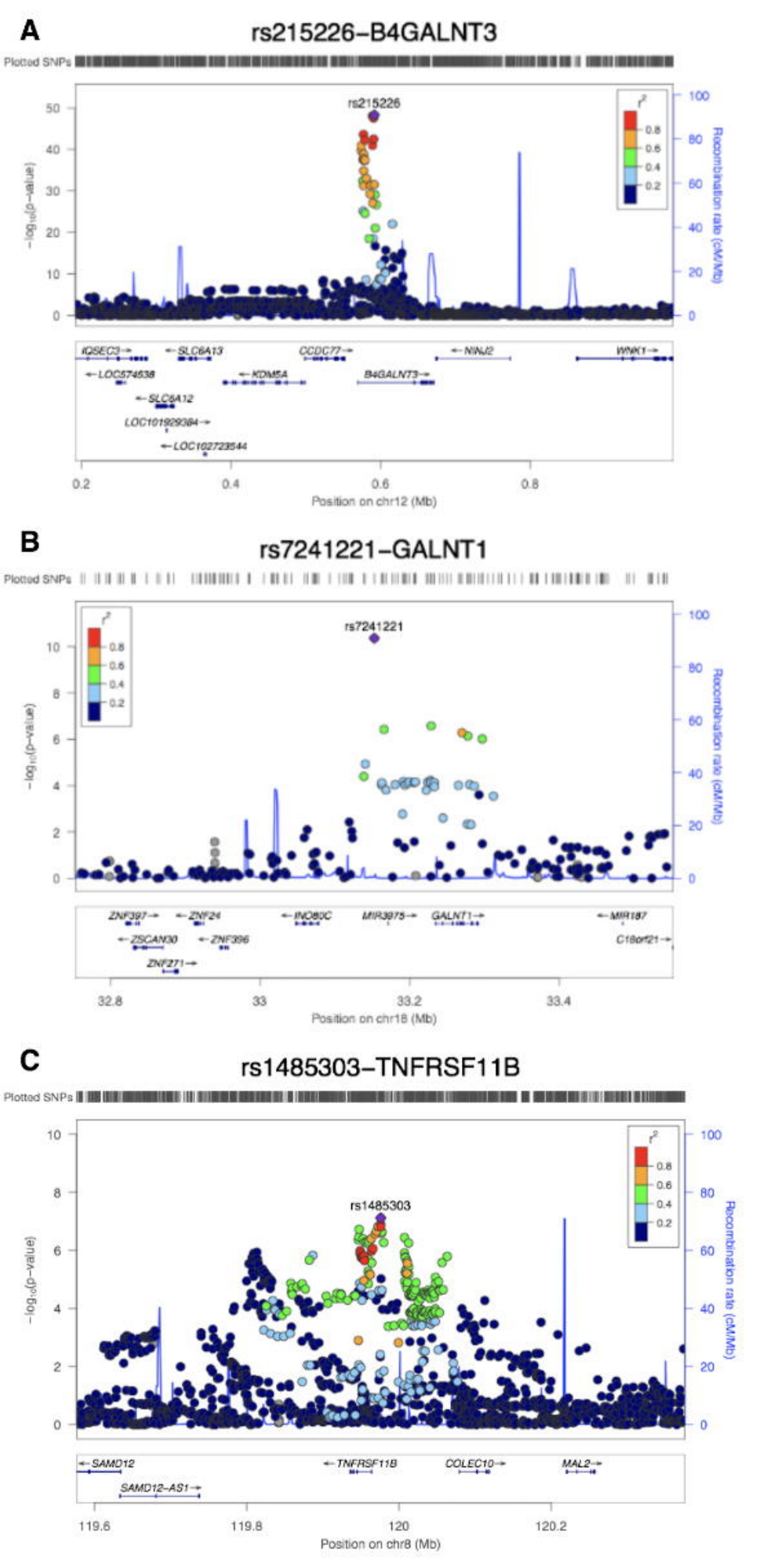
A
rs215226–B4GALNT3
Plotted SNPs
rs215226
−log10(p-value)
Recombination rate (cM/Mb)
r²
0.8
0.6
0.4
0.2
IQSEC3→
←SLC6A13
CCDC77→
←NINJ2
WNK1→
←LOC574538
←KDM5A
B4GALNT3→
←SLC6A12
LOC101929384→
←LOC102723544
0.2
0.4
0.6
0.8
Position on chr12 (Mb)
B
rs7241221–GALNT1
Plotted SNPs
rs7241221
−log10(p-value)
Recombination rate (cM/Mb)
r²
0.8
0.6
0.4
0.2
ZNF397→
←ZNF24
←INO80C
MIR3975→
GALNT1→
←MIR187
←ZSCAN30
←ZNF396
C18orf21→
ZNF271→
32.8
33
33.2
33.4
Position on chr18 (Mb)
C
rs1485303–TNFRSF11B
Plotted SNPs
rs1485303
−log10(p-value)
Recombination rate (cM/Mb)
r²
0.8
0.6
0.4
0.2
←SAMD12
←TNFRSF11B
COLEC10→
MAL2→
SAMD12-AS1→
119.6
119.8
120
120.2
Position on chr8 (Mb)

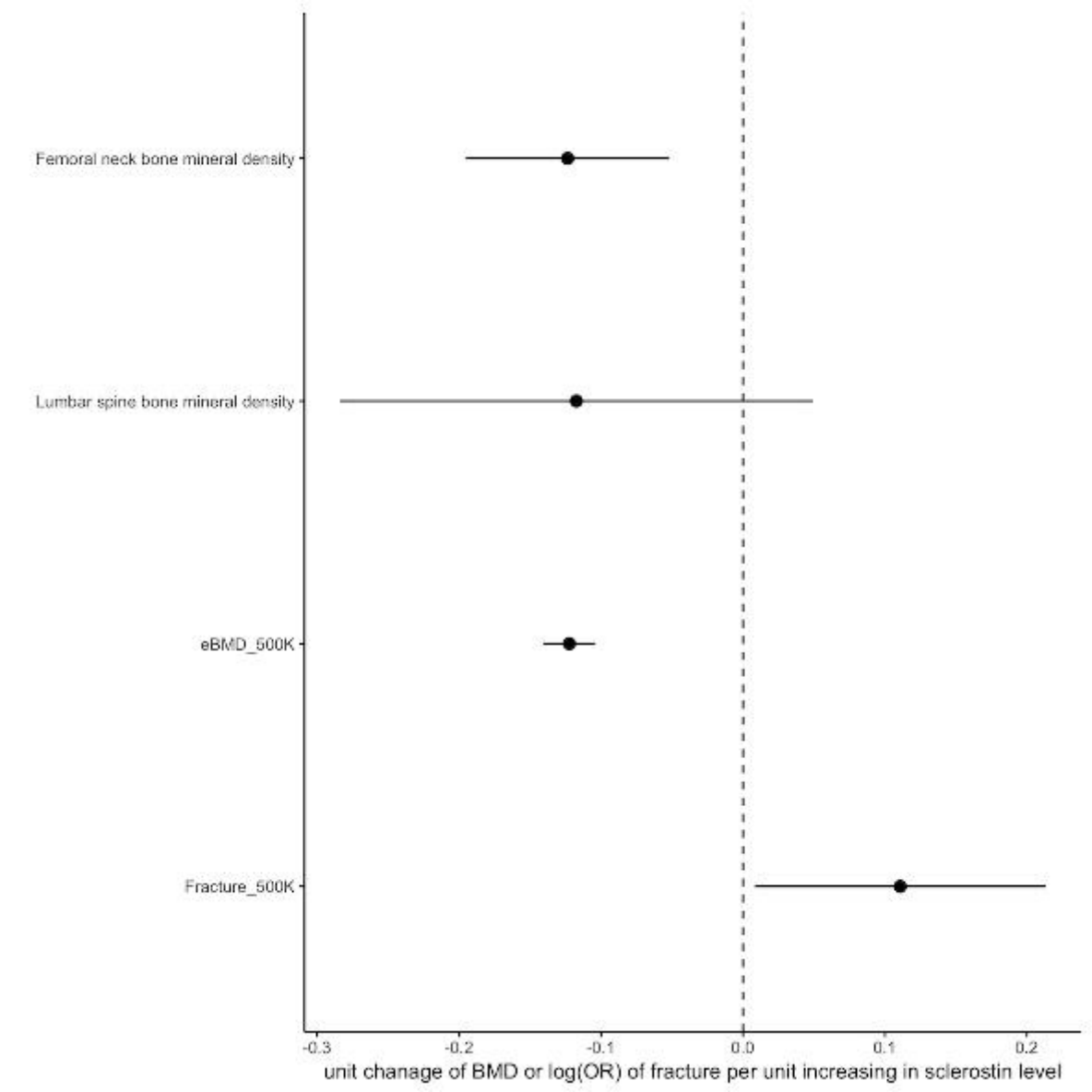
Femoral neck bone mineral density
Lumbar spine bone mineral density
eBMD_500K
Fracture_500K
-0.3
-0.2
-0.1
0.0
0.1
0.2
unit chanage of BMD or log(OR) of fracture per unit increasing in sclerostin level

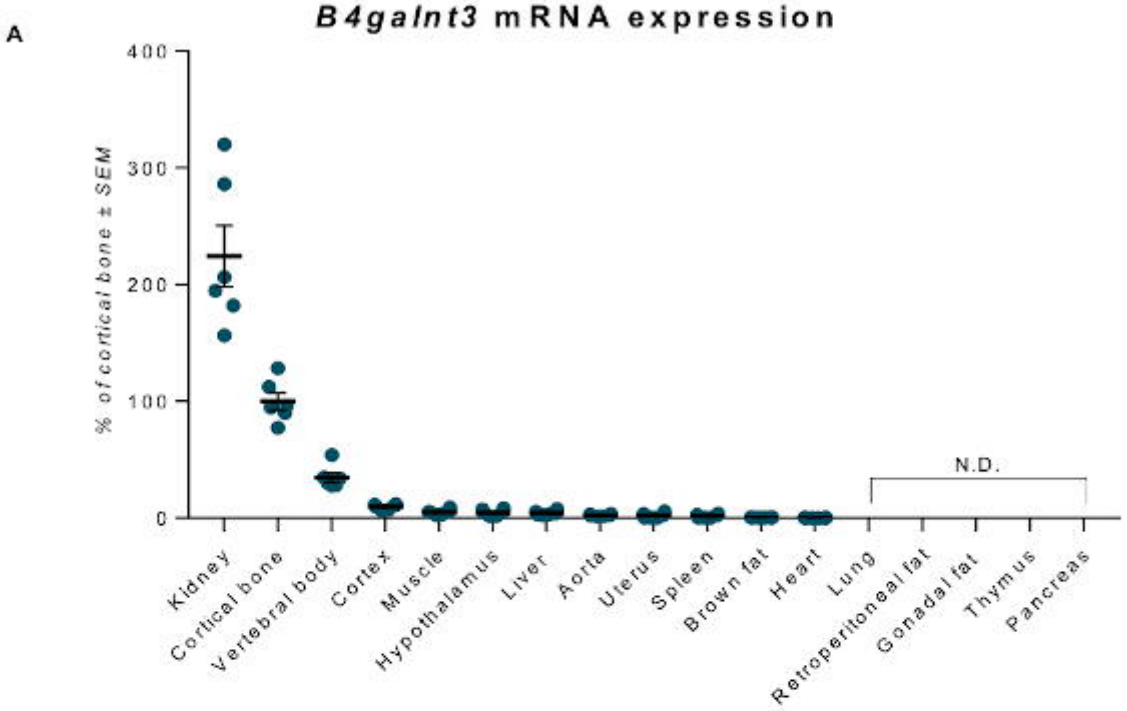
A
B4galnt3 mRNA expression
% of cortical bone ± SEM
400
300
200
100
0
N.D.
Kidney
Cortical bone
Vertebral body
Cortex
Muscle
Hypothalamus
Liver
Aorta
Uterus
Spleen
Brown fat
Heart
Lung
Retroperitoneal fat
Gonadal fat
Thymus
Pancreas

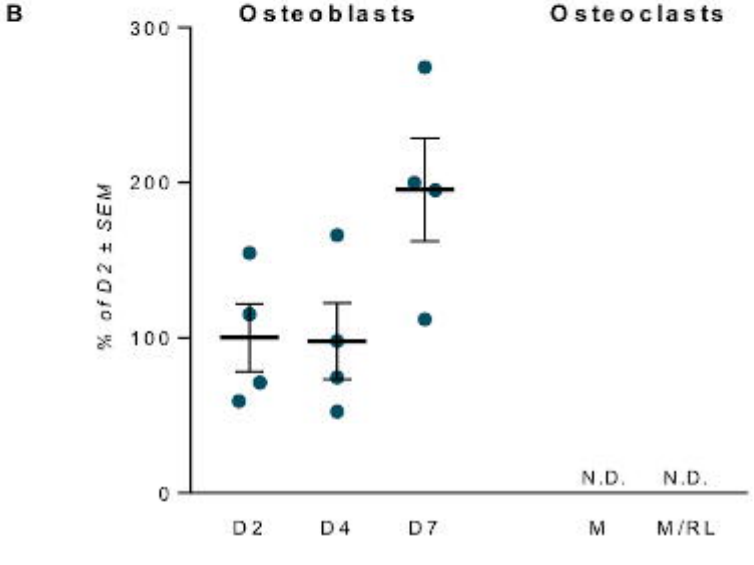
B
Osteoblasts
Osteoclasts
% of D2 ± SEM
300
200
100
0
N.D.
N.D.
D2
D4
D7
M
M/RL

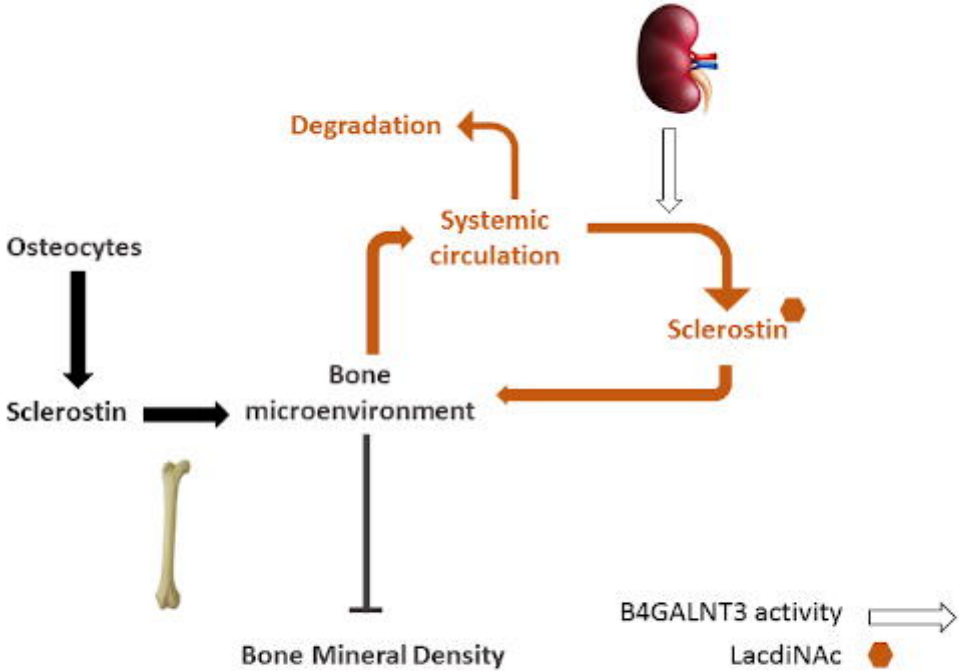
Degradation
Systemic circulation
Osteocytes
Sclerostin
Bone microenvironment
Sclerostin
Bone Mineral Density
B4GALNT3 activity
LacdiNAc